Received October 14, 2021, accepted October 26, 2021, date of publication November 8, 2021, date of current version November 12, 2021.

*Digital Object Identifier 10.1109/ACCESS.2021.3126311*

# Spiking Neural Network Discovers Energy-Efficient Hexapod Motion in Deep Reinforcement Learning

**KATSUMI NAYA, KYO KUTSUZAWA, (Member, IEEE), DAI OWAKI, (Member, IEEE), AND MITSUHIRO HAYASHIBE, (Senior Member, IEEE)**

Neuro-Robotics Laboratory, Department of Robotics, Graduate School of Engineering, Tohoku University, Sendai 980-8579, Japan

Corresponding author: Mitsuhiro Hayashibe (mitsuhiro.hayashibe@inria.fr)

This work was supported by the JSPS Grant-in-Aid for Scientific Research on Innovative Areas Hyper-Adaptability Project under Grant 20H05458.

**ABSTRACT** In Deep Reinforcement Learning (DRL) for robotics application, it is important to find energy-efficient motions. For this purpose, a standard method is to set an action penalty in the reward to find the optimal motion considering the energy expenditure. This method is widely used for the simplicity of implementation. However, since the reward is a linear sum, if the penalty is too large, the system will fall into local minima and no moving solution can be obtained. In contrast, if the penalty is too small, the effect may not be sufficient. Therefore, it is necessary to adjust the amount of the penalty so that the agent always moves dynamically, and the energy-saving effect is sufficient. Nevertheless, since adjusting the hyperparameters is computationally expensive, we need a learning method that is robust to the penalty setting problem. We investigated on the Spiking Neural Network (SNN), which has been attracting attention for its computational efficiency and neuromorphic architecture. We conducted gait experiments using a hexapod agent while varying the energy penalty settings in the simulation environment. By applying SNN to the conventional state-of-the-art DRL algorithms, we examined whether the agent could explore for an optimal gait with a larger penalty variation and obtain an energy-efficient gait verified with Cost of Transport (CoT), a metric of energy efficiency for gait. Soft Actor-Critic (SAC)+SNN resulted in a CoT of 1.64, Twin Delayed Deep Deterministic policy gradient (TD3)+SNN resulted in a CoT of 2.21, and Deep Deterministic policy gradient (DDPG)+SNN resulted in a CoT of 2.08 (1.91 for normal SAC, 2.38 for TD3, and 2.40 for DDPG). DRL combined with SNN succeeded in learning more energy efficient gait with lower CoT.

**INDEX TERMS** Spiking neural network, deep reinforcement learning, energy efficiency, hexapod gait, spatio-temporal backpropagation.

## I. INTRODUCTION

Energy-efficient control is an important aspect in the field of robotics as the energy resource is limited for autonomous mobile robots. Several studies have been conducted to minimize the energy consumption of legged robots. One method changes the gait to match the terrain using CPG [1] and other methods transit the gait according to its own energy consumption [2], [3]. On the other hand, Deep Reinforcement Learning (DRL), which learns the optimal behavior under unknown environments by end-to-end learning, has recently attracted considerable attention in robotics for its high capability on solution space exploration.

In DRL, it adopts another approach to obtain energy-efficient behavior patterns by learning. One standard way is to add an action penalty term to the reward function by multiplying the agent's action by a weight coefficient for considering the energy expenditure. This method can be practically applied to any DRL algorithm because it only adds a term to the reward function, and it is reported to be effective in preventing overfitting [4]. However, the weight coefficients need to be somewhat larger to achieve a sufficient effect. Because the reward is a linear sum, if the penalty is too large, the system falls into local minima, and no moving solution can be obtained. In contrast, if the penalty is too

The associate editor coordinating the review of this manuscript and approving it for publication was Frederico Guimarães.

small, the effect may be insufficient. Therefore, adjusting the hyperparameters generally requires many trials, and the computational cost and manual tuning effort become a central issue of the DRL technique. In the motion generation task using continuous control, it is necessary to search for a control input that enables dynamic movement at all times. Besides, we need a learning method that is robust to the reward setting problem without falling into the local minima where the agent stops, even if we penalize the energy expenditure.

To overcome these issues, we investigated a spiking neural network (SNN), which has attracted attention for its computational efficiency and neuromorphic architecture. An SNN is a model of neurons in the brain that transmits information by spiking signals. It can handle spatio-temporal information, and in biological systems, noise induces the generation of regularity in excitable systems such as neurons and cells [5]. An SNN has discontinuous potentials and contains noise in the system. Therefore, it is expected to yield better results [6], [7]. The spikes are binary and do not need to transmit analog values; thus, SNNs can perform efficient computation [8], [9], and recently, it has been reported that they can rapidly search for movements that adapt to the environment during walking motions [10]. The potential for higher exploration performance of SNNs can be an attractive function for the learning process. However, this exploration ability aspect of SNNs has not been well studied in robotics so far, compared to other well-known aspects.

In this study, we performed walking experiments with a larger penalty variation for a hexapod agent and with the state-of-the-art different DRL algorithms. We verify whether the combination of DRL and SNNs can explore the optimal motion and obtain energy-efficient behavior patterns, even when the energy penalty is larger than that for conventional DRL. In addition to the investigation of its reward acquisition, we also verified the cost of transport (CoT), which is a metric of energy efficiency for gait.

## II. RELATED WORK

SNNs have been focused on their ability to perform efficient computations because of their ability to handle binary spikes. Thus, several studies have already been performed to apply SNNs to mobile robots [11]–[13]. However, it is known that the backpropagation method used in artificial neural networks (ANNs) cannot be applied to the training of SNNs; thus, spike-timing-dependent plasticity (STDP) was used to train SNNs in these studies. STDP performs well only in low-dimensional tasks, but it has difficulty in high-dimensional tasks. SNNs use other learning rules to solve high-dimensional tasks, and some methods have been proposed, such as converting a trained ANN into an SNN [14], which approximates the backpropagation method of an ANN (SpikeProp [15], SuperSpike [16], spatio-temporal Backpropagation [17]). In a study using these learning methods to tackle high-dimensional continuous control tasks, a method of applying SNNs to DRL algorithms was proposed [18], [19]. They applied SNNs to the actor part of each DRL algorithm and used ANNs for the critic. They also showed that they were able to deploy to Loihi, a neuromorphic processor, and performed efficient computation.

In contrast, although these studies focused on the benefit of efficient computation, another point of view is that the discontinuous potential of the model contributes to the robustness of the model [7]. Furthermore, a musculoskeletal biped simulation study was reported [10] that enabled immediate adaptation to environmental changes in its gait by using an SNN-based controller with the contribution of spike-induced ordering.

## III. BACKGROUND

In this section, we describe a brief reinforcement-learning problem setup and the algorithm we used. Next, we describe the concept of spiking neural networks (SNNs), model, and PopSAN, which combines DRL and SNNs.

### A. DEEP REINFORCEMENT LEARNING

In DRL problems, we consider an infinite-horizon Markov decision process (MDP), defined by $(\mathcal{S}, \mathcal{A}, p, r)$, where the state space $\mathcal{S}$ and the action space $\mathcal{A}$ are continuous, the state transition probability $p : \mathcal{S} \times \mathcal{S} \times \mathcal{A} \rightarrow [0, 1]$ represents the probability density function of the current state $s_t$ and action $a_t$ to the next state $s_{t+1}$, and $r : \mathcal{S} \times \mathcal{A} \rightarrow \mathcal{R}$ represents the reward given by interacting with the environment. In addition, we use trajectory $\rho_\pi$ that is obtained by the policy $\pi(a_t|s_t)$.

We used three different model-free DRL algorithms, SAC [20], TD3 [21], and DDPG [22], which are widely used in continuous control tasks. SAC and TD3 are now known as state-of-the-art DRL algorithms.

SAC is a stochastic DRL algorithm that learns a policy $\pi(a_t|s_t)$ that maximizes the objective function (1) considering the entropy term $\mathcal{H}$ of the policy.

$$J(\pi) = \sum_{t=0}^{\infty} E_{(s_t,a_t)\sim\rho_\pi} \left[ r\left(s_t, a_t\right) + \gamma \cdot H\left(\pi\left(\cdot \mid s_t\right)\right)\right] \quad (1)$$

By maximizing the expected policy entropy term, the learned policy can maximize the reward obtained while maintaining the diversity of the behaviors for better exploration ability. In addition, it can be trained off-policy, resulting in high sample efficiency. More details of the theorem are provided in [20].

TD3 and DDPG are deterministic DRL algorithms that learn policy $\pi(a_t|s_t) = \mu_\theta(s)$ that outputs the presumably optimal action for the current state. TD3 improves the exploration ability and overestimation of the estimated value. The objective function is shown in Equation (2).

$$J(\pi) = \sum_{t=0}^{\infty} E_{(s_t,a_t)\sim\rho_\pi} \left[ r\left(s_t, a_t\right)\right] \quad (2)$$

In TD3, an overestimation of the value estimated in the DDPG is improved by using a method called clipped double Q-learning, which extends the double Q-learning in discrete actions. In addition, to improve the exploration capability,

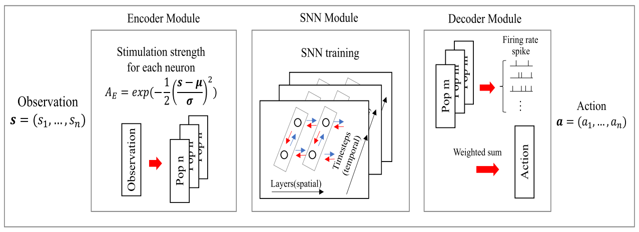

**FIGURE 1.** Global architecture of PopSAN.

Gaussian noise is added to the output of the deterministic policy (target policy smoothing).

### B. SPIKING NEURAL NETWORK

SNNs transmit information through spike trains. Besides, it captures the characteristics of real spiking neurons. Various models have been proposed [23], [24], [25]. The spike train is shown in (3).

$$S(t) = \sum_{s} \delta(t - t^s) \tag{3}$$

where s is the label of a spike and $\delta$ is a Dirac function.

One of the most widely used models is the leaky integrate-and-fire (LIF) model for its computational simplicity. The LIF model is described in Equation (4).

$$\tau \frac{du(t)}{dt} = -u(t) + I(t) \tag{4}$$

where $u(t)$ is the membrane potential at time $t$, $\tau$ is the time constant and $I(t)$ is input signal that is induced by a presynaptic spike train. When membrane potential $u(t)$ exceeds a given threshold $V_{th}$, the neuron fires and resets its potential to $u_{reset}$.

Although SNNs have the advantage of handling spatio-temporal information, it is known that the backpropagation of an ANN cannot be applied directly to the training of multi-layered SNNs. Thus, we used the STBP method [17], which has shown high performance in SNN training.

### C. PopSAN

In this study, we applied SNN to DRL using the PopSAN method [19]. Fig.1 shows the architecture of PopSAN.

PopSAN is an application of SNNs to the actor part of the actor-critic in reinforcement learning and consists of an encoder module, a computation module of an SNN, and a decoder module. In the encoder module, the observation is encoded as a spike using population coding. The stimulation strength in the population, $A_E$, is expressed by Equation (5).

$$\boldsymbol{A_E} = \exp\left(-1/2 \cdot ((\boldsymbol{s} - \boldsymbol{\mu})/\boldsymbol{\sigma})^2\right) \tag{5}$$

After being converted to the spike format, the SNN is trained using extended STDP [18]. LIF neurons were used in the SNN module. First, the presynaptic spike $o$ is integrated and converted to a current $c$ (6). The current $c$ is then integrated and converted to a membrane potential $v$ (7). When the membrane potential exceeds a threshold, the neuron fires (8).

$$\boldsymbol{c}(t) = d_c \cdot \boldsymbol{c}(t-1) + \boldsymbol{W} \cdot \boldsymbol{o}(t) + \boldsymbol{b} \tag{6}$$

$$\boldsymbol{v}(t) = d_v \cdot \boldsymbol{v}(t-1) \cdot (1 - \boldsymbol{o}(t-1)) + \boldsymbol{c}(t) \tag{7}$$

$$\boldsymbol{o}(t) = Threshold(\boldsymbol{v}(t)) \tag{8}$$

$d_c$ and $d_v$ are the current and voltage decay factors.

The decoder module converts the activity of the population output of the SNN layer into the action of the agent. It calculates the firing rate by summing up the number of spikes of the neurons in each defined timestep (9). Then, the $i^{th}$ action is calculated using Equation (10).

$$\boldsymbol{fr} = \frac{\sum_{t=1}^{T} \boldsymbol{o}(t)}{T} \tag{9}$$

$$\boldsymbol{a} = \boldsymbol{W_d} \cdot \boldsymbol{fr} + \boldsymbol{b_d} \tag{10}$$

$W_d$ and $b_d$ are weight and bias for each action dimension.

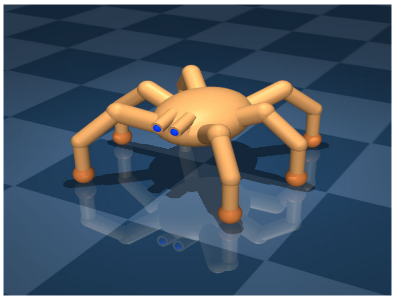

**FIGURE 2.** Hexapod agent in our study. It has observations as the joint positions and velocities, torso velocities and orientations, and sensor information (IMU, force, torque). Actions are input to the actuator of each joint.

## IV. PROPOSED METHOD

We conducted walking experiments with DRL and SNN-driven DRL, and compared the results with the cost of transport (CoT), a measure of energy efficiency.

In this section, we explain the details of the agents used in the walking experiment, PopSAN, which applies SNNs to DRL, and the details of CoT.

### A. SIMULATED AGENTS

We carried out experiments using MuJoCo [26], a physics simulation engine that is widely used for reinforcement learning of continuous control tasks. We chose a legged robot that is widely used as a mobile robot. The hexapod agent is shown in Fig. 2 and was created in the dm_control [27] environment, an open-source library by DeepMind. The agent has six legs. For each leg, the shoulder has two degrees of freedom of rotation, the elbow has one degree of freedom of rotation, and the wrist has one degree of freedom of linear motion, which is a passive spring. Three actuators for drive the shoulder and elbow. The joints of the agent are set with certain stiffness, so that the posture is maintained even when no torque is applied. However when it walks, the agent needs

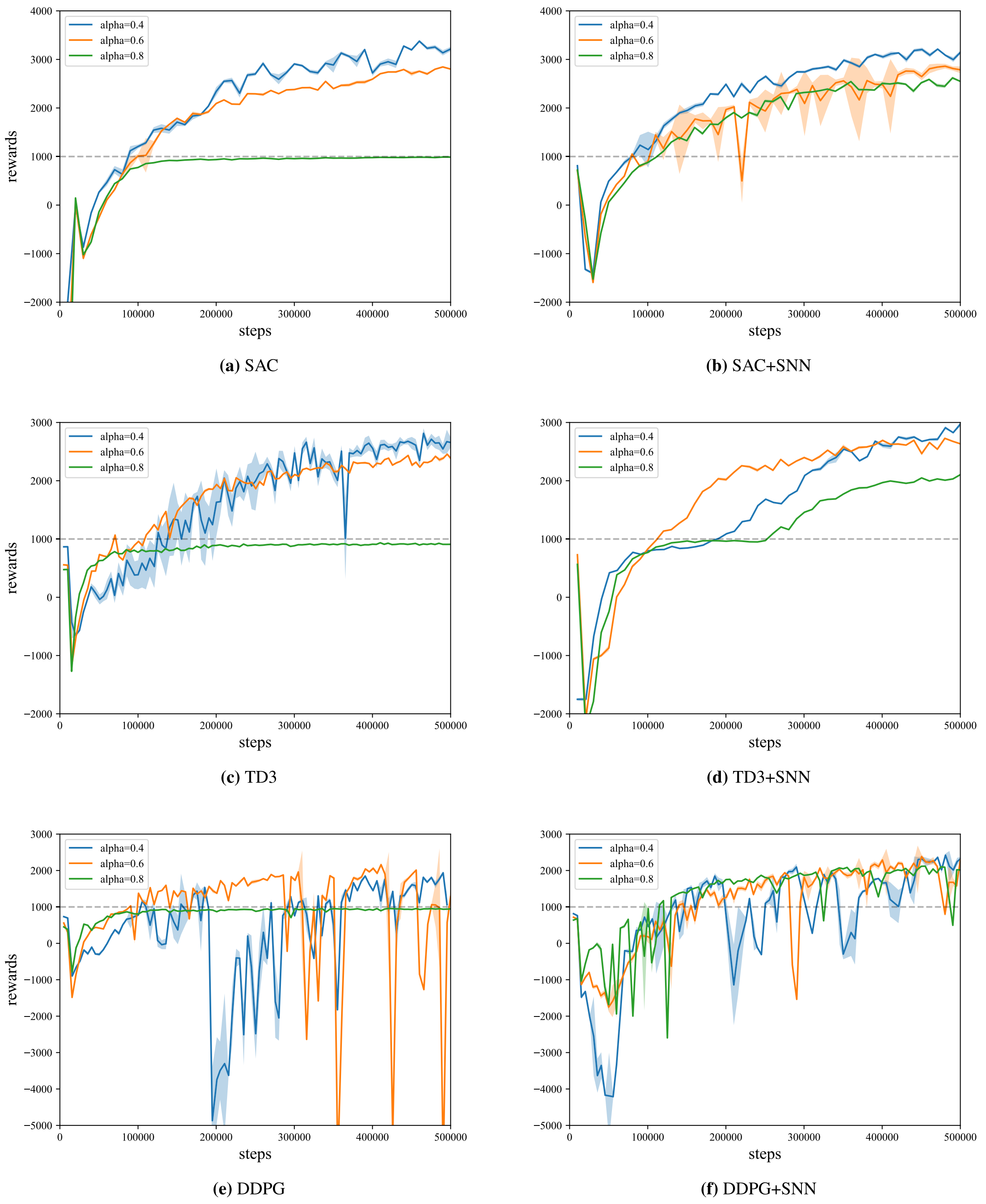

**(a)** SAC **(b)** SAC+SNN **(c)** TD3 **(d)** TD3+SNN **(e)** DDPG **(f)** DDPG+SNN

**FIGURE 3.** For each algorithm, the temporal variation regarding reward during the learning is visualized while the value of $\alpha$ is varied from 0 to 1. 1 rollout is 1000 timesteps. If an the reward converges at 1000 (the dotted line), it indicates that the agent is stopped for walking.

to apply torque to move its body. These are 112 observations: the position and velocity of the hinge, the output of the torque of the actuators, the velocity of the torso, the uprightness of the torso (the inner product of the z-axis of the torso and the z-axis of the absolute coordinate), the value of the IMU sensor, and the force and torque applied to the toes. Actions have 18 dimensions: the torque input of each leg actuator.

**TABLE 1.** **The training results for each algorithm at 200k and 500k steps. The reward is the value obtained by subtracting the survival reward from the reward used in training. SD represents the standard deviation for 10 evaluations.**

| | | α | 0.0 | 0.2 | 0.4 | 0.6 | 0.8 | 1.0 |
|---|---|---|---|---|---|---|---|---|
| SAC | 200k step | Reward | 5174 | 1635 | 1340 | 1092 | -26.8 | -68.3 |
| | | SD | 59.78 | 116.92 | 88.57 | 17.82 | 0.47 | 0.31 |
| | 500k step | Reward | **5532** | 3032 | **2214** | **1801** | 449.4 | -15.8 |
| | | SD | 44.12 | 43.03 | 45.22 | 15.80 | 2.53 | 0.00 |
| TD3 | 200k step | Reward | 1348 | 543.9 | 527.5 | 865.8 | -153.6 | -130.5 |
| | | SD | 56.81 | 578.75 | 144.09 | 12.30 | 0.79 | 0.99 |
| | 500k step | Reward | 3428 | 1176 | 1657 | **1387** | -82.7 | -126.1 |
| | | SD | 242 | 572 | 85.83 | 12.01 | 0.85 | 0.50 |
| DDPG | 200k step | Reward | 203.9 | 381.7 | -65.9 | 375.1 | -131.7 | -58.5 |
| | | SD | 23.66 | 234.22 | 39.09 | 16.49 | 2.16 | 0.89 |
| | 500k step | Reward | 1168 | **1831** | 61.1 | 282.8 | -54.7 | -47.9 |
| | | SD | 650.59 | 119.33 | 282.37 | 211.08 | 0.51 | 0.26 |
| SAC+SNN | 200k step | Reward | 4641 | 2699 | 1488 | 967.0 | 880.6 | -55.1 |
| | | SD | 46.36 | 339.09 | 27.64 | 61.71 | 7.92 | 0.92 |
| | 500k step | Reward | 5369 | **3832** | 2144 | 1787 | **1465** | -17.7 |
| | | SD | 30.11 | 37.30 | 37.00 | 70.46 | 22.49 | 0.00 |
| TD3+SNN | 200k step | Reward | 1056 | 1406 | 91.0 | 551.4 | -83.5 | -145.9 |
| | | SD | 1065 | 629.0 | 3.73 | 21.35 | 0.79 | 0.84 |
| | 500k step | Reward | **4634** | **2405** | **1971** | 1276 | **331.1** | -146.1 |
| | | SD | 89.67 | 164.22 | 43.39 | 32.64 | 4.06 | 0.45 |
| DDPG+SNN | 200k step | Reward | 157.5 | 356.7 | 674.0 | 611.1 | 750.9 | -141.1 |
| | | SD | 15.80 | 90.80 | 86.27 | 16.63 | 9.14 | 0.52 |
| | 500k step | Reward | **1386** | 1680 | **1315** | **758.6** | **1017** | -83.7 |
| | | SD | 652.49 | 62.13 | 58.80 | 52.71 | 29.73 | 0.21 |

**TABLE 2.** **Cost of Transport (CoT) obtained from each algorithm. red indicates less than 2.5, bold indicates greater than or equal to 2.5 and less than 3.0. X indicates the situation where the agent did not walk.**

| | | α | 0.0 | 0.2 | 0.4 | 0.6 | 0.8 | 1.0 |
|---|---|---|---|---|---|---|---|---|
| SAC | 200k step | CoT | 3.123 | 3.487 | **2.768** | **2.099** | X | X |
| | | SD | 0.059 | 0.024 | 0.043 | 0.028 | | |
| | 500k step | CoT | 3.320 | **2.796** | **2.425** | **1.913** | **2.550** | X |
| | | SD | 0.042 | 0.027 | 0.017 | 0.039 | 0.013 | |
| TD3 | 200k step | CoT | 7.522 | 3.419 | **2.678** | **2.406** | X | X |
| | | SD | 0.477 | 0.288 | 0.034 | 0.021 | | |
| | 500k step | CoT | 3.621 | 3.766 | **2.942** | **2.378** | X | X |
| | | SD | 0.151 | 0.115 | 0.067 | 0.021 | | |
| DDPG | 200k step | CoT | 12.240 | 5.475 | 17.395 | **2.591** | X | X |
| | | SD | 1.161 | 1.458 | 11.426 | 0.085 | | |
| | 500k step | CoT | 5.556 | 3.887 | **2.709** | **2.397** | X | X |
| | | SD | 0.896 | 0.079 | 0.043 | 0.028 | | |
| SAC+SNN | 200k step | CoT | 3.916 | 3.752 | **2.586** | **2.159** | **2.354** | X |
| | | SD | 0.123 | 0.060 | 0.030 | 0.058 | 0.023 | |
| | 500k step | CoT | 3.483 | 3.421 | **2.415** | **1.900** | **1.640** | X |
| | | SD | 0.560 | 0.024 | 0.035 | 0.035 | 0.017 | |
| TD3+SNN | 200k step | CoT | 4.875 | 3.964 | **2.761** | **2.268** | **2.639** | X |
| | | SD | 0.832 | 0.137 | 0.080 | 0.015 | 0.028 | |
| | 500k step | CoT | 4.339 | 3.588 | **2.951** | **2.207** | **2.430** | X |
| | | SD | 0.127 | 0.139 | 0.064 | 0.014 | 0.019 | |
| DDPG+SNN | 200k step | CoT | 9.665 | 4.439 | 3.233 | **2.699** | **2.175** | X |
| | | SD | 0.836 | 0.250 | 0.375 | 0.707 | 0.012 | |
| | 500k step | CoT | 3.948 | **2.994** | **2.801** | **2.259** | **2.077** | X |
| | | SD | 0.960 | 0.088 | 0.113 | 0.034 | 0.019 | |

We set the reward function $R$ as in (11) and trained the agents using each algorithm.

$$R = v + s - \alpha \sum_{i=0}^{actuator} a_i(t)^2 \tag{11}$$

where $v$ is the speed of the torso, $s$ is the survival reward, which takes the value 1 for each time step until it falls, $a_i(t)$ is the torque input to the actuator (action) and $\alpha$ is the coefficient for the sum of the squares of action over the number of actuators. $\alpha$ acts as a penalty for the energy expenditure. As the action penalty increases, the agent is required to acquire more energy-efficient walking patterns.

## B. WALKING EXPERIMENT

We trained the agent using each of the DRL algorithms and SNN-driven DRL algorithms. We chose PopSAN [19] as the method for adapting an SNN to each DRL algorithm. The DRL algorithm that we used was based on PFRL [28], a DRL library. We also implemented PopSAN in combination with DRL of PFRL, referring to the authors' implementation.[1] The source code used in this study can be found at [2] We used a DNN and an SNN with 256 neurons in two layers. The other hyperparameters are described in Table. 3.

## C. COST OF TRANSPORT

We used the energy efficiency metric, CoT, to evaluate the efficiency of walking obtained through learning to verify the physical performance rather than the computational reward.

[1]https://github.com/combra-lab/pop-spiking-deep-rl
[2]https://github.com/Katsumi-N/hexapod_walk_snn

CoT is defined as (12).

$$CoT = \frac{\sum_{i=0} \int_0^t |a_i(t)\dot{\theta}_i(t)|dt}{mg\Delta d} \tag{12}$$

where the numerator is the energy consumption of the agent, $a_i(t)$ and $\theta_i(t)$ indicate the torque input and angle of the $i^{th}$ joint, respectively. $m$ is the mass of the agent, $g$ is gravity, and $\Delta d$ is the distance traveled by the agent. The CoT indicates the amount of energy required to move a unit distance, and the smaller the CoT, the greater the energy-efficiency of walking.

## V. EXPERIMENTAL RESULT

To obtain more energy-efficient walking, we trained the agent using the DRL algorithms SAC, TD3, DDPG, and each algorithm with SNN, by varying the reward setting regarding the value of the weighting factor for energy expenditure $\alpha$ from 0 to 1. Subsequently, to evaluate the energy efficiency of the walking obtained from the training, we measured the CoT of a trained agent.

## A. WALKING EXPERIMENT

Table 1 shows the final reward for the walking experiment, which is calculated as the total reward minus the survival reward. Fig. 3 shows the learning process. We set 1000 timesteps for a rollout, and every 10 000 timesteps, 10 evaluations without exploration are run. We trained each algorithm for 500 000 timesteps using three seeds. SD is the standard deviation of the reward over 10 evaluations. If the agent falls down in the middle of the learning process, it starts the next rollout. The highest reward for each algorithm with and without the SNNs is shown in red. This means there is one red indication between SAC and SAC+SNN, one red

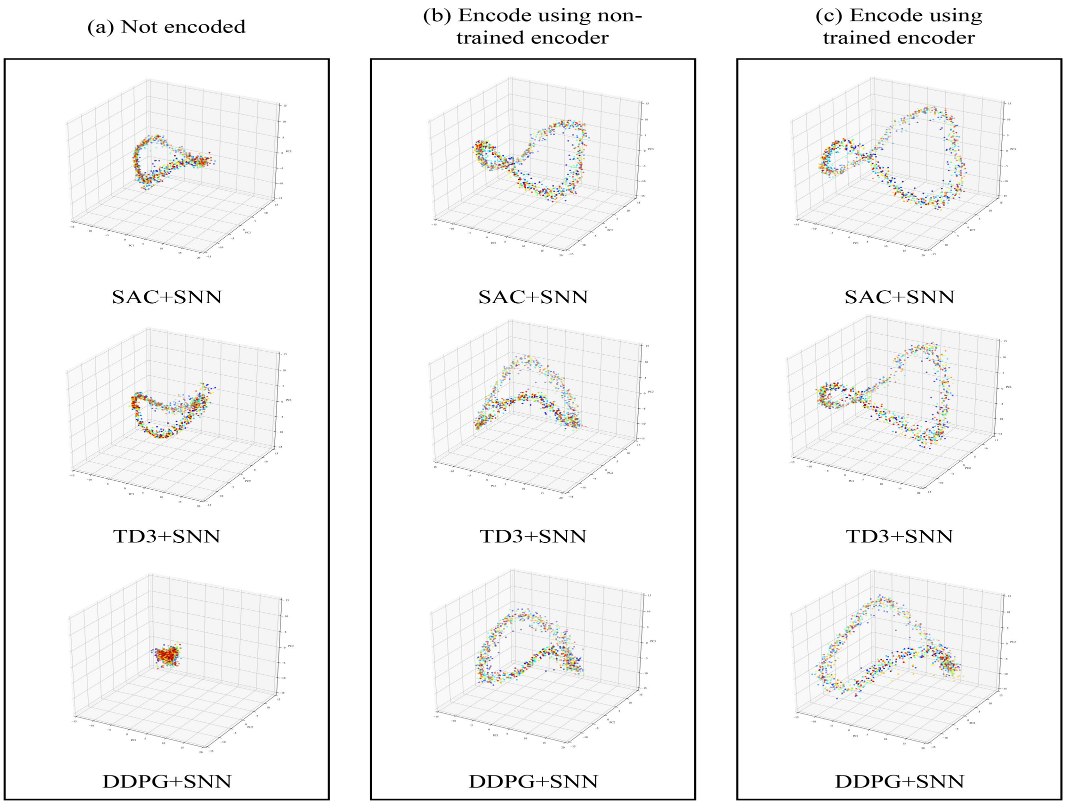

**FIGURE 4.** Results of PCA on the gait of trained agent's observations at 1000 timesteps. (a) shows observations after training (500 000 timesteps) without encoding. (b) shows observations encoded into spike format with the non-trained encoder. (c) shows observations encoded with the trained encoder. In (c), the observations are more separated than in (a) and (b).

indication between TD3 and TD3+SNN and so on. Here, for each algorithm, as the value $\alpha$ increases, the total reward collected is 1000, indicate that no walking progress has been made. When the robot stops, the first term (velocity) and the third term (penalty for the action) of the reward equation become zero, and only the second term (the survival reward) is given. The maximum number of timesteps is 1000 if the robot does not fall over, so the reward for stopping the robot is 1000. the agent is learning to stop. In each DRL, the reward did not exceed 1000 at $\alpha = 0.8$, and the agent stopped without walking. In contrast, DRL with an SNN succeeded in learning walking with a reward higher than 1000 in each case.

## B. MEASURING THE COST OF TRANSPORT

Next, we measured the CoT using the agent that had trained for 200 000 timesteps and 500 000 timesteps, as shown in Table 2. We performed 1000 timestep walking experiments 30 times to calculate the CoT and its standard deviation. Red and bold letters indicate CoT less than 2.5, and within the range of 2.5–3, respectively. Table 2 reveals that, in most cases, the CoT decreased as the learning step progressed. As $\alpha$ increased, the agent was able to learn more energy-efficient walking with a lower CoT. The results show that it is effective to increase the penalty term of the action to learn an efficient movement. For SAC+SNN and DDPG+SNN, walking with the smallest CoT was obtained when $\alpha = 0.8$. For each algorithm, the DRL with SNN obtained a lower CoT walking than the DRL alone.

Fig. 5-7 shows the position and velocity of the center of mass (CoM) in the z-axis (height direction) during the last learning phase for 1000 timesteps of walking for each algorithm at $\alpha = 0.6$. In the case of TD3 and DDPG, the temporal variation of the phase portrait was largely reduced by using the SNN and a consistent limit cycle based on the CoM. By using the SNN, the agent was able to learn to walk with less CoM shift, which is an energy-efficient walking with low CoT.

## C. ANALYSIS OF ENCODED OBSERVATIONS

To validate the SNN contributions to the acquisition of gait patterns, we examined how the agent's observations were separated into spikes during encoding.

For each algorithm using the SNN, we performed principal component analysis on the observations of the agent with 500 000 timestep training (a), the observations encoded into spike format using an untrained encoder (b), and the observations encoded using a trained encoder (c). The PCA results are presented in Fig. 4. Regarding (a) and (b), even when untrained encoders are used, they are transformed into a form that captures more periodic structures than the unencoded

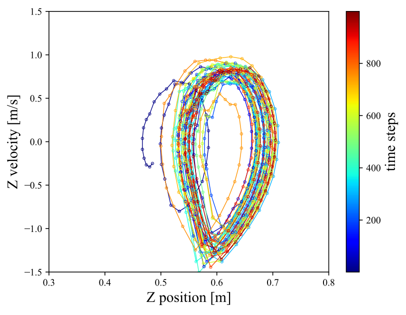

**(a)** SAC

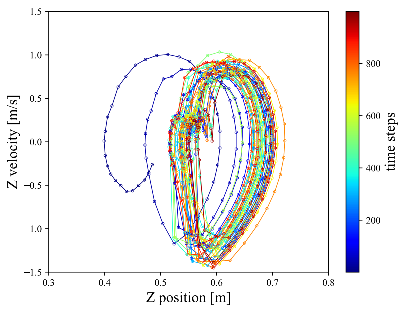

**(b)** SAC+SNN

**FIGURE 5.** **Phase portrait regarding CoM for SAC and SAC+SNN at $\alpha = 0.6$. This figure shows the relationship between the position of the CoM on the z-axis (height direction) and its velocity for the last learning phase (1000 timesteps).**

**TABLE 3.** **Hyperparameters for each DRL algorithms.**

| Algorithm | SAC | TD3 | DDPG |
|---|---|---|---|
| Actor(Policy) | 256-ReLU-256-ReLU-Gaussian_head | 256-ReLU-256-ReLU-Tanh_head | 256-ReLU-256-ReLU-Tanh_head |
| Actor(PopSAN) | 256-LIF-256-LIF-Out pop | 256-LIF-256-LIF-Out pop | 256-LIF-256-LIF-Out pop |
| Critic(Q function) | 256-ReLU-256-ReLU-Linear | 256-ReLU-257-ReLU-Linear | 256-ReLU-258-ReLU-Linear |
| Learning Rate(Policy) | 0.0003 | 0.0005 | 0.0003 |
| Learning Rate(PopSAN) | 0.0003 | 0.0003 | 0.0005 |
| Batch size | 256(128 when α=0.8) | 256 | 256 |

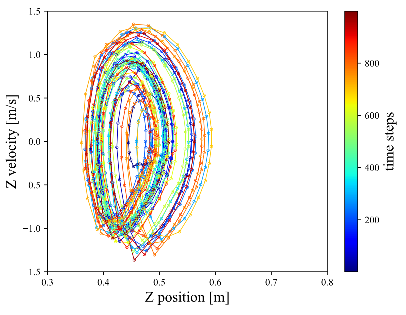

**(a)** TD3

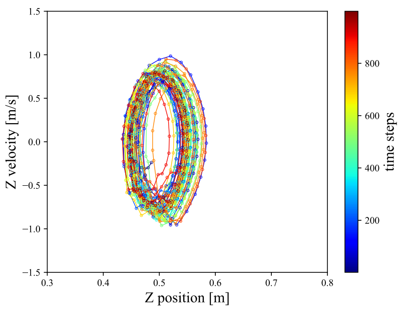

**(b)** TD3+SNN

**FIGURE 6.** **Phase portrait of CoM for TD3 and TD3+SNN at $\alpha = 0.6$.**

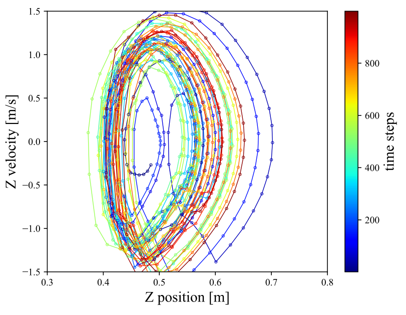

**(a)** DDPG

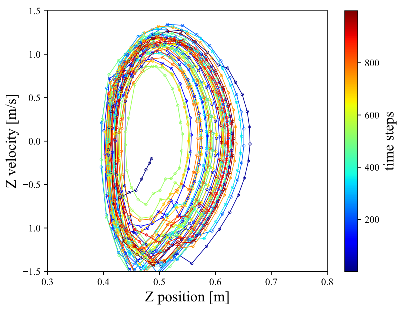

**(b)** DDPG+SNN

**FIGURE 7.** **Phase portrait of CoM for DDPG and DDPG+SNN at $\alpha = 0.6$.**

observations, especially DDPG+SNN. Furthermore, when regarding (b) and (c), before and after learning the encoder, the distance between the observations in (c) is greater than that in (b). It is thought that the learning of the encoder has improved the representational capability of the network, and thus, the observations can better be separated. These results suggest that the learned encoder transforms its observations into a complex and periodic structure through learning, which is advantageous for learning gait

## VI. DISCUSSION

As shown in Table 2, by using the SNN in all algorithms of SAC, TD3, and DDPG, the agent was able to learn walking without falling into the local minima of stopping at $\alpha = 0.8$. In contrast, when $\alpha = 0.8$, it could not learn walking by using TD3 and DDPG. It walked by using SAC but with a high CoT. In addition, for the same value of $\alpha$, the algorithms with the SNN exhibited a lower CoT than that without the SNN. Thus, we were able to obtain energy-efficient behavior patterns with low CoTs. Among all these tests, SAC+SNN achieved the lowest CoT of 1.64. This result is significant because SAC is already known for its good exploration ability; however, it can

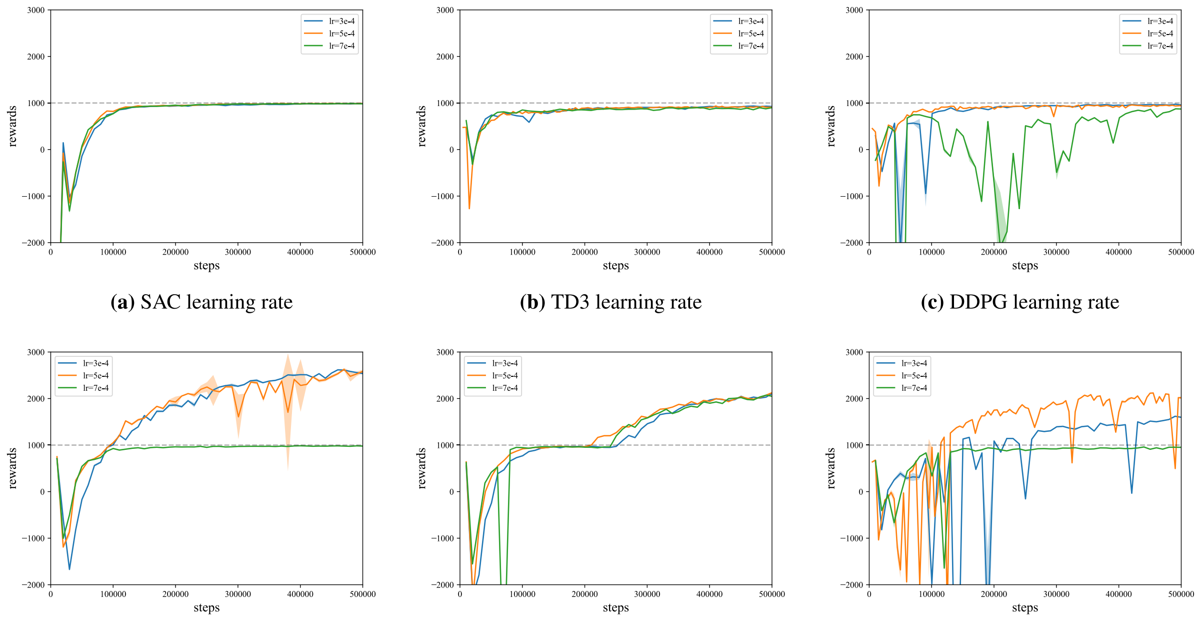

**(a)** SAC learning rate **(b)** TD3 learning rate **(c)** DDPG learning rate

**(d)** SAC+SNN learning rate **(e)** TD3+SNN learning rate **(f)** DDPG+SNN learning rate

**FIGURE 8. Learning rate validation of hyperparameters when $\alpha = 0.8$.**

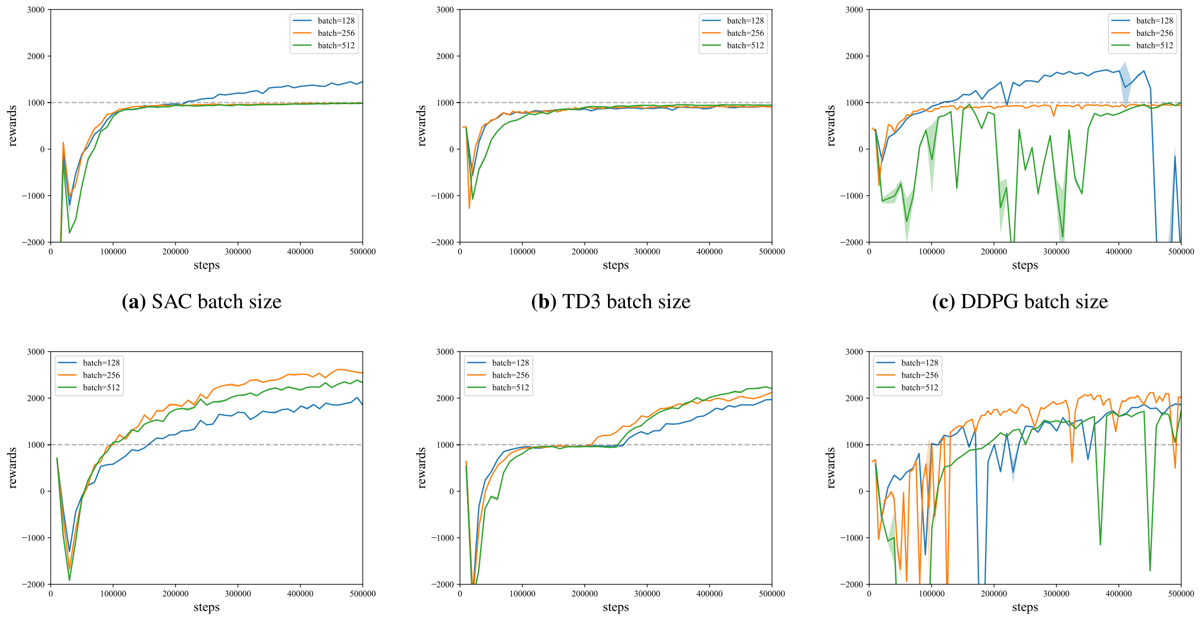

**(a)** SAC batch size **(b)** TD3 batch size **(c)** DDPG batch size

**(d)** SAC+SNN batch size **(e)** TD3+SNN batch size **(f)** DDPG+SNN batch size

**FIGURE 9. Batch size validation of hyperparameters when $\alpha = 0.8$.**

be further improved by combining it with an SNN. The good exploration ability of SAC could be confirmed when it was compared to TD3 and DDPG. Although DDPG did not show good performance, it was more effective when combined with the SNN. This can be observed from the numbers of bold and red rewards and CoT in the tables, as compared to the case of non-SNN DDPG.

SAC is known to have a higher exploration ability than other deterministic DRL algorithms, and it was reported to produce more energy-efficient motions than TD3 in our group's previous study [29], [30]. However, this is the first report on the case where the most energy-efficient gait was obtained when SAC was combined SAC with SNN. Potentially, this indicates that the type of exploration can be different and compensatory for both the SAC and SNN explorations. In addition, Fig. 3 and Table 1 show that gait patterns in TD3 and DDPG driven by SNNs are less variable than those without SNNs, resulting in an increasing trend in reward. Because these algorithms learn by deterministic policy, they exhibit fast computations; however, compared to algorithms such as SAC, they tend to fall into local minima.

Therefore, SNN facilitated the acquisition of periodic patterns, which in turn led to the acquisition of gait patterns with less CoM shift, as shown in Figs.6 and- 7. This probably results from obtaining a more accurate periodic representation of the observations via population coding, an shown in Fig. 4. In particular, DDPG showed a sudden drop in reward in the later stages of learning; however, by using SNN, the model acquired a more stable gait, which is a visible improvement incorporated with SNN.

In DDPG and TD3, noise is added to improve the exploration performance, but the size of the noise is a hyperparameter, so it needs to be adjusted for each task to obtain a sufficient effect. However, the noise effect caused by the discontinuous potentials of the SNN does not require hyperparameter adjustment; therefore, it can be used generally for various DRL algorithms.

In contrast, the CoT is sometimes lower for normal DRLs when either the learning step or $\alpha$ is small. In PopSAN, both the encoders and decoders are learnable. However, when the learning steps are small, they are not learned sufficiently, which may result in high CoT walking. The reason why the CoT is sometimes lower in normal DRL when $\alpha$ is small is that the influence of the energy efficiency term in the reward is small, and even SNN-driven DRL sometimes results in a gait with unnecessarily large leg movements.

## VII. CONCLUSION

In this study, to obtain energy-efficient gait patterns, we trained a six-legged agent to walk with different reward settings by varying the weight to consider for the energy expenditure. The effect of SNN-driven DRL was investigated over different DRL algorithms and evaluated for the energy efficiency of the hexapod gait using CoT.

In both the stochastic algorithm such as SAC and the deterministic algorithm such as TD3 and DDPG, we succeeded in searching the walking pattern even with a larger energy penalty setting, when it was combined with SNN. SNN-driven DRL obtained a more energy-efficient gait when the learning step was considerable, and a larger energy penalty was set. To the best of our knowledge, this is the first report that the most energy-efficient motion could be obtained when SAC is driven with an SNN than with SAC only. In addition, we confirmed the increase in the reward in TD3 and DDPG.

Until now, SNNs have been mainly focused on their computational efficiency merits, but we have experimentally demonstrated that they are also beneficial in terms of acquiring periodic patterns for energy-efficient motor learning in legged agents in DRL.

## APPENDIX
## HYPERPARAMETERS FOR EACH DRL ALGORITHMS

The hyperparameters used for each DRL algorithm are listed in Table 3. Some parameters that significantly affected the learning were experimentally determined by the validation experiments shown in Figs. 8 and 9. The other parameters were determined by referring to PFRL [28] and PopSAN [19].

Fig. 8 shows that none of the DRL algorithms succeed in learning. On the contrary, SNN-driven DRL succeeds in learning, except when the learning rate is 7e-4 in SAC+SNN and DDPG+SNN. Fig. 9 shows that all batch sizes, except when the SAC's batch size is 128, fail to learn, whereas the SNN-driven DRL succeeds in learning for all batch sizes.

## REFERENCES

[1] S. Zenker, E. E. Aksoy, D. Goldschmidt, F. Worgotter, and P. Manoonpong, "Visual terrain classification for selecting energy efficient gaits of a hexapod robot," in *Proc. IEEE/ASME Int. Conf. Adv. Intell. Mechatronics*, Jul. 2013, pp. 577–584.

[2] G. Wang, L. Ding, H. Gao, Z. Deng, Z. Liu, and H. Yu, "Minimizing the energy consumption for a hexapod robot based on optimal force distribution," *IEEE Access*, vol. 8, pp. 5393–5406, 2020.

[3] N. Kottege, C. Parkinson, P. Moghadam, A. Elfes, and S. P. N. Singh, "Energetics-informed hexapod gait transitions across terrains," in *Proc. IEEE Int. Conf. Robot. Autom. (ICRA)*, May 2015, pp. 5140–5147.

[4] J.-C. Shi, Y. Yu, Q. Da, S.-Y. Chen, and A.-X. Zeng, "Virtual-taobao: Virtualizing real-world online retail environment for reinforcement learning," in *Proc. AAAI Conf. Artif. Intell.*, Jul. 2019, vol. 33, no. 1, pp. 4902–4909. [Online]. Available: https://ojs.aaai.org/index.php/AAAI/article/view/4419

[5] B. Lindner, J. Garcia-Ojalvo, A. Neiman, and L. Schimansky-Geier, "Effects of noise in excitable systems," *Phys. Rep.*, vol. 392, no. 6, pp. 321–424, 2004. [Online]. Available: https://www.sciencedirect.com/science/article/pii/S0370157303004228

[6] N. Kasabov and E. Capecci, "Spiking neural network methodology for modelling, classification and understanding of EEG spatio-temporal data measuring cognitive processes," *Inf. Sci.*, vol. 294, pp. 565–575, Feb. 2015. [Online]. Available: https://www.sciencedirect.com/science/article/pii/S0020025514006562

[7] J. H. Lee, T. Delbruck, and M. Pfeiffer, "Training deep spiking neural networks using backpropagation," *Frontiers Neurosci.*, vol. 10, p. 508, Nov. 2016. [Online]. Available: https://www.frontiersin.org/article/10.3389/fnins.2016.00508

[8] E. Z. Farsa, A. Ahmadi, M. A. Maleki, M. Gholami, and H. N. Rad, "A low-cost high-speed neuromorphic hardware based on spiking neural network," *IEEE Trans. Circuits Syst. II, Exp. Briefs*, vol. 66, no. 9, pp. 1582–1586, Sep. 2019.

[9] B. V. Benjamin, P. Gao, and E. McQuinn, "Neurogrid: A mixed-analog-digital multichip system for large-scale neural simulations," *Proc. IEEE*, vol. 102, no. 5, pp. 699–716, May 2014.

[10] S. Yonekura and Y. Kuniyoshi, "Spike-induced ordering: Stochastic neural spikes provide immediate adaptability to the sensorimotor system," *Proc. Nat. Acad. Sci. USA*, vol. 117, no. 22, pp. 12486–12496, Jun. 2020. [Online]. Available: https://www.pnas.org/content/117/22/12486

[11] Z. Bing, C. Meschede, G. Chen, A. Knoll, and K. Huang, "Indirect and direct training of spiking neural networks for end-to-end control of a lane-keeping vehicle," *Neural Netw.*, vol. 121, pp. 21–36, Jan. 2020. [Online]. Available: https://www.sciencedirect.com/science/article/pii/S0893608019301595

[12] G. Tang, A. Shah, and K. P. Michmizos, "Spiking neural network on neuromorphic hardware for energy-efficient unidimensional slam," in *Proc. IEEE/RSJ Int. Conf. Intell. Robots Syst. (IROS)*, Nov. 2019, pp. 4176–4181.

[13] A. S. Lele, Y. Fang, J. Ting, and A. Raychowdhury, "Learning to walk: Spike based reinforcement learning for hexapod robot central pattern generation," in *Proc. 2nd IEEE Int. Conf. Artif. Intell. Circuits Syst. (AICAS)*, Aug. 2020, pp. 208–212.
[14] D. Patel, H. Hazan, D. J. Saunders, H. T. Siegelmann, and R. Kozma, "Improved robustness of reinforcement learning policies upon conversion to spiking neuronal network platforms applied to atari breakout game," *Neural Netw.*, vol. 120, pp. 108–115, Dec. 2019. [Online]. Available: https://www.sciencedirect.com/science/article/pii/S0893608019302266
[15] S. Bohte, J. Kok, and J. Poutre, "SpikeProp: Backpropagation for networks of spiking neurons," in *Proc. ESANN*, vol. 48, Jan. 2000, pp. 419–424.
[16] F. Zenke and S. Ganguli, "SuperSpike: Supervised learning in multilayer spiking neural networks," *Neural Comput.*, vol. 30, no. 6, pp. 1514–1541, Jun. 2018.
[17] Y. Wu, L. Deng, G. Li, J. Zhu, and L. Shi, "Spatio-temporal backpropagation for training high-performance spiking neural networks," *Frontiers Neurosci.*, vol. 12, p. 331, May 2018. [Online]. Available: https://www.frontiersin.org/article/10.3389/fnins.2018.00331
[18] G. Tang, N. Kumar, and K. P. Michmizos, "Reinforcement co-learning of deep and spiking neural networks for energy-efficient mapless navigation with neuromorphic hardware," in *Proc. IEEE/RSJ Int. Conf. Intell. Robots Syst. (IROS)*, Oct. 2020, pp. 1–8.
[19] G. Tang, N. Kumar, R. Yoo, and K. P. Michmizos, "Deep reinforcement learning with population-coded spiking neural network for continuous control," in *Proc. 4th Conf. Robot Learn. (CoRL)*, 2020, pp. 1–10.
[20] T. Haarnoja, A. Zhou, P. Abbeel, and S. Levine, "Soft actor-critic: Off-policy maximum entropy deep reinforcement learning with a stochastic actor," in *Proc. Int. Conf. Mach. Learn. (ICML)*, 2018, pp. 1861–1870.
[21] S. Fujimoto, H. van Hoof, and D. Meger, "Addressing function approximation error in actor-critic methods," in *Proc. Int. Conf. Mach. Learn.*, 2018, pp. 1587–1596.
[22] T. P. Lillicrap, J. J. Hunt, A. Pritzel, N. Heess, T. Erez, Y. Tassa, D. Silver, and D. Wierstra, "Continuous control with deep reinforcement learning," in *Proc. 4th Int. Conf. Learn. Represent. (ICLR)*, Y. Bengio and Y. LeCun, Eds., San Juan, PR, USA, 2016.
[23] A. L. Hodgkin and A. F. Huxley, "A quantitative description of membrane current and its application to conduction and excitation in nerve," *J. Physiol.*, vol. 117, no. 4, pp. 500–544, Aug. 1952, doi: 10.1113/jphysiol.1952.sp004764.
[24] A. N. Burkitt, "A review of the integrate-and-fire neuron model: I. homogeneous synaptic input," *Biol. Cybern.*, vol. 95, no. 1, pp. 1–19, Jul. 2006.
[25] E. M. Izhikevich, "Which model to use for cortical spiking neurons?" *IEEE Trans. Neural Netw.*, vol. 15, no. 5, pp. 1063–1070, Sep. 2004.
[26] E. Todorov, T. Erez, and Y. Tassa, "MuJoCo: A physics engine for model-based control," in *Proc. IEEE/RSJ Int. Conf. Intell. Robots Syst.*, Oct. 2012, pp. 5026–5033.
[27] Y. Tassa, S. Tunyasuvunakool, A. Muldal, Y. Doron, S. Liu, S. Bohez, J. Merel, T. Erez, T. Lillicrap, and N. Heess, "dm_control: Software and tasks for continuous control," *Softw. Impacts*, vol. 6, Nov. 2020, Art. no. 100022.
[28] Y. Fujita, T. Kataoka, P. Nagarajan, and T. Ishikawa, "Chainerrl: A deep reinforcement learning library," in *Proc. Workshop Deep Reinforcement Learn. 33rd Conf. Neural Inf. Process. Syst.*, Dec. 2019, pp. 1–14.
[29] J. Chai and M. Hayashibe, "Motor synergy development in high-performing deep reinforcement learning algorithms," *IEEE Robot. Autom. Lett.*, vol. 5, no. 2, pp. 1271–1278, Apr. 2020.
[30] J. Han, J. Chai, and M. Hayashibe, "Synergy emergence in deep reinforcement learning for full-dimensional arm manipulation," *IEEE Trans. Med. Robot. Bionics*, vol. 3, no. 2, pp. 498–509, May 2021.

**KATSUMI NAYA** received the B.E. degree from the Department of Mechanical and Aerospace Engineering, Tohoku University, Japan, in 2020. He is currently pursuing the M.S. degree with the Neuro-Robotics Laboratory, Graduate School of Biomedical Engineering, Tohoku University. His research interests include deep reinforcement learning, spiking neural networks, and machine learning.

**KYO KUTSUZAWA** (Member, IEEE) received the B.E. degree in electrical and electronic systems and the M.E. and Dr.Eng. degrees in science and engineering from Saitama University, Japan, in 2015, 2017, and 2020, respectively. He is currently an Assistant Professor at Tohoku University. His research interests include robotics, motion generation, force signal processing, and neural networks. He received the Advanced Robotics Excellent Paper Award, in 2020, and the Young Investigation Excellence Award from the Robotics Society of Japan, in 2018.

**DAI OWAKI** (Member, IEEE) received the Ph.D. degree from the Department of Electrical and Communication Engineering, Graduate School of Engineering, Tohoku University, in 2009. From April 2009 to March 2011, he was an Assistant Professor with the Graduate School of Engineering, Tohoku University. From April 2011 to September 2017, he was an Assistant Professor with the Research Institute of Electrical Communication, Tohoku University. From October 2017 to March 2019, he was an Assistant Professor with the Department of Robotics, Graduate School of Engineering, Tohoku University. Since April 2019, he has been an Associate Professor with the Department of Robotics, Graduate School of Engineering, Tohoku University. His main research interests include neurorobotics, synthetic neuro-rehabilitation, and bio-hybrid systems. He received the 2008 IEEE Robotics and Automation Society Japan Chapter Young Award (ICRA 2008), the SICE Annual Conference Young Author's Award, in 2008, and the Young Scientists Award, MEXT, in 2020.

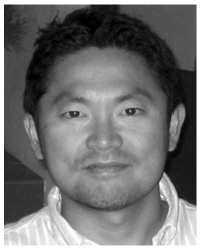

**MITSUHIRO HAYASHIBE** (Senior Member, IEEE) received the B.S. degree from the Tokyo Institute of Technology, in 1999, and the M.S. and Ph.D. degrees from the Graduate School of Engineering, The University of Tokyo, in 2001 and 2005, respectively. He was an Assistant Professor with the Department of Medicine, Jikei University School of Medicine, from 2001 to 2006. He was a Postdoctoral Fellow at the Institute National de Recherche en Informatique et en Automatique (INRIA), and the Laboratoire d'Informatique, de Robotique, de Microelectronique de Montpellier (LIRMM), CNRS/the University of Montpellier, France, in 2007. Since 2008, he has been a Tenured Research Scientist with INRIA and the University of Montpellier. He has also been a Visiting Researcher at the RIKEN Brain Science Institute and TOYOTA Collaboration Center, since 2012. He has been a Professor at the Department of Robotics, Tohoku University, and the Founder of the Neuro-Robotics Laboratory, since 2017. He is a Senior Member of the IEEE Engineering in Medicine and Biology Society. He serves as a Technical Activity Board Member for the International Foundation of Robotics Research (IFRR). He was a recipient of the 15th Annual Delsys Prize 2017 for Innovation in Electromyography from the De Luca Foundation, USA.

• • •